


Magnetic fluctuations in $\text{Pb}_9\text{Cu}(\text{PO}_4)_6\text{O}$ Makoto Shimizu ^{1,*}, Junya Otsuki ², and Harald O. Jeschke ²¹*Department of Physics, Graduate School of Science, Kyoto University, Kyoto 606-8502, Japan*²*Research Institute for Interdisciplinary Science, Okayama University, Okayama 700-8530, Japan*

(Received 28 August 2023; revised 11 October 2023; accepted 24 October 2023; published 8 November 2023)

The hope that copper-doped lead apatite $\text{Pb}_9\text{Cu}(\text{PO}_4)_6\text{O}$ is a room-temperature superconductor has largely been dashed by global research efforts. Nevertheless, the material has interesting magnetic properties, and research groups around the world have prepared high-quality samples. We use a fluctuation exchange (FLEX) approximation approach to study the magnetic tendencies in $\text{Pb}_9\text{Cu}(\text{PO}_4)_6\text{O}$. We find ferromagnetic (FM) fluctuations very close to the filling of the stoichiometric compound which can be understood from Fermi surface nesting at the M point. This is like the one-band triangular lattice Hamiltonian at $\frac{3}{4}$ filling. Interestingly, the special k_z dependence of the $\text{Pb}_9\text{Cu}(\text{PO}_4)_6\text{O}$ band structure makes it very sensitive to doping. Only slight charge doping switches between antiferromagnetic and ferromagnetic fluctuations. If the material could become superconducting, it might be easily switchable between singlet and triplet superconductivity.

DOI: [10.1103/PhysRevB.108.L201105](https://doi.org/10.1103/PhysRevB.108.L201105)

Introduction. Copper-doped lead apatite $\text{Pb}_9\text{Cu}(\text{PO}_4)_6\text{O}$ has recently been put forward as a candidate for room-temperature superconductivity at ambient pressure [1,2], causing substantial excitement in the scientific community. Efforts at independent synthesis of the material and reproduction of experimental observations have been undertaken by many groups [3–5]. Every failure to reproduce superconductivity [6] has added to doubts concerning the interpretation of the original experiments. However, the suggestion that a well-known phase transition in Cu_2S [7], which is a known impurity [1], is responsible for the sudden change in resistivity at 104 K in the mixed-phase $\text{Pb}_9\text{Cu}(\text{PO}_4)_6\text{O}$ samples is rather convincing [8]. Nevertheless, it is still an interesting question what the properties of the impurity-free $\text{Pb}_9\text{Cu}(\text{PO}_4)_6\text{O}$ material are. The half levitation [2] that has been reproduced by some groups [5,9] points to interesting magnetic properties. The fact that excellent single crystals of $\text{Pb}_9\text{Cu}(\text{PO}_4)_6\text{O}$ have been grown [10] means that this question is now accessible to precise experiments.

The experimental claims for $\text{Pb}_9\text{Cu}(\text{PO}_4)_6\text{O}$ have been met with a concerted response of the theoretical materials science community. Very fast density functional theory (DFT) studies [11–15] have discussed the importance of flat bands and the shape of the Fermi surface. Several different tight-binding models have been proposed [13,16,17] and analyzed with respect to topological properties [18]. Authors of three DFT + dynamical mean-field theory (DMFT) studies have shown that, at the integer filling of the stoichiometric $\text{Pb}_9\text{Cu}(\text{PO}_4)_6\text{O}$ compound, correlations open a gap [19–21], in agreement with the transparent single crystals [10]. Superconductivity has been theoretically studied using the two-dimensional (2D) $t - J$ model [22] and spin-fluctuation theory [23]. Some state-

ments about the magnetism of $\text{Pb}_9\text{Cu}(\text{PO}_4)_6\text{O}$ have been obtained [24].

In this paper, we study the magnetic fluctuations in Cu-doped $\text{Pb}_{10}(\text{PO}_4)_6\text{O}$ using the fluctuation exchange (FLEX) approximation [25,26]. The stoichiometric $\text{Pb}_9\text{Cu}(\text{PO}_4)_6\text{O}$ compound is described by a $\frac{3}{4}$ -filled two-orbital model. Its Fermi surface has been described as rugby ball shaped. We take the three-dimensional (3D) nature of the compound seriously and work out the similarity and differences between the electronic structure of $\text{Pb}_9\text{Cu}(\text{PO}_4)_6\text{O}$ and a one-band model at different fillings on the triangular lattice.

Electronic structure. We perform all-electron DFT calculations for $\text{Pb}_9\text{Cu}(\text{PO}_4)_6\text{O}$ using the full potential local orbital (FPLO) basis [27] and the generalized gradient approximation (GGA) exchange-correlation functional [28]. We derive a precise four-band tight-binding model using the symmetry-conserving projected Wannier functions implemented within FPLO [29].

We base our model of the structure of $\text{Pb}_9\text{Cu}(\text{PO}_4)_6\text{O}$ on the crystal structure of lead apatite $\text{Pb}_{10}(\text{PO}_4)_6\text{O}$ as determined by Krivovichev and Burns [30]. Its $P6_3/m$ (No. 176) space group has an $O(4)$ position that is only occupied by one quarter. We first simplify by choosing one of four symmetry-equivalent $O(4)$ positions which reduces the symmetry to $P3$ (No. 143). According to Ref. [13], the $\text{Pb}(2)$ position with four symmetry-equivalent sites is energetically more favorable for Cu substitution. We thus replace one out of four Pb atoms by Cu and perform an internal relaxation of this structure. As DFT structure prediction has well-known issues for correlated oxides, we use experimental [1] rather than DFT-predicted lattice parameters. The resulting crystal structure is shown in Fig. 1(a). It is like the structures considered in other works [13,31]. There are some variations in the electronic structures that have been obtained for $\text{Pb}_9\text{Cu}(\text{PO}_4)_6\text{O}$; this may be due to different ways of symmetry reduction, placement of Cu, and structural relaxation as well as differences in DFT basis

*shimizu.makoto.5c@kyoto-u.ac.jp

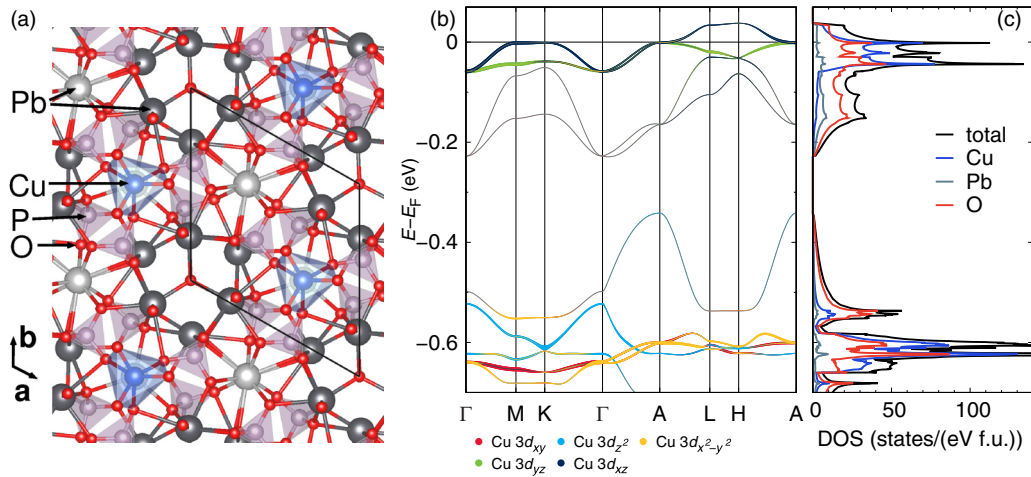


FIG. 1. (a) Predicted simplified crystal structure of $\text{Pb}_9\text{Cu}(\text{PO}_4)_6\text{O}$. (b) Electronic band structure and (c) density of states near the Fermi level at the generalized gradient approximation (GGA) level with Cu $3d$ orbital character highlighted.

sets and convergence. We have been careful to follow an established structure modeling recipe [13,20,23] and use a highly converged all-electron DFT approach. We expect the conclusions we draw from the electronic structures presented here to be equally valid for the electronic structures discussed in many other works on $\text{Pb}_9\text{Cu}(\text{PO}_4)_6\text{O}$.

We show the DFT band structure and density of states of $\text{Pb}_9\text{Cu}(\text{PO}_4)_6\text{O}$ in Figs. 1(b) and 1(c). Two almost degenerate bands of Cu $3d_{xz}$ and $3d_{yz}$ character cross the Fermi level. They are slightly hybridizing with two occupied oxygen bands arising from the extra O in the formula, the O(4) in the $\text{Pb}_{10}(\text{PO}_4)_6\text{O}$ structure; this has also been observed in Ref. [31]. Therefore, in this paper, we work with a four-band tight-binding model. The upper of the two bands at the Fermi level leads to the 3D Fermi surface shown in Fig. 2(c). It has a Mount Fuji shape because the finite k_z dispersion leads to different filling levels of the underlying triangular lattice at every value of k_z . Slight hole doping [Figs. 2(b) and 2(a)] leads to the rugby ball shape that has been found previously [11] and to tiny Fermi surfaces from the second Cu $3d$ band. The shape remains qualitatively the same between undoped and moderate electron doping [Fig. 2(d)]. This k_z dispersion

of the electronic structure will constitute the main difference from a fully 2D triangular lattice Hamiltonian.

We determine [29] a four-band tight-binding model including $3d_{xz}$ and $3d_{yz}$ orbitals of Cu and $2p_x$ and $2p_y$ orbitals of O. The Hamiltonian \mathcal{H}_0 is given by

$$\mathcal{H}_0 = \sum_{ij\mu\sigma} t_{ij}^{\mu\nu} c_{i\mu\sigma}^\dagger c_{j\nu\sigma}, \quad (1)$$

where i and j are site indices, μ and ν are orbital indices, and σ is the spin index. The occupation number is $n = 7$ for the stoichiometric $\text{Pb}_9\text{Cu}(\text{PO}_4)_6\text{O}$. Three bands are fully occupied, and the top band is half-filled without doping and interactions. This means that, at stoichiometry, one band forms the Fermi surface. However, the two upper bands deriving almost entirely from Cu $3d$ are nearly degenerate, and the orbital character of the bands and Fermi surface changes between $3d_{xz}$ and $3d_{yz}$ depending on the k direction.

Spin fluctuations. To discuss spin fluctuations, we consider interactions between $3d$ electrons on Cu. We adopt the usual

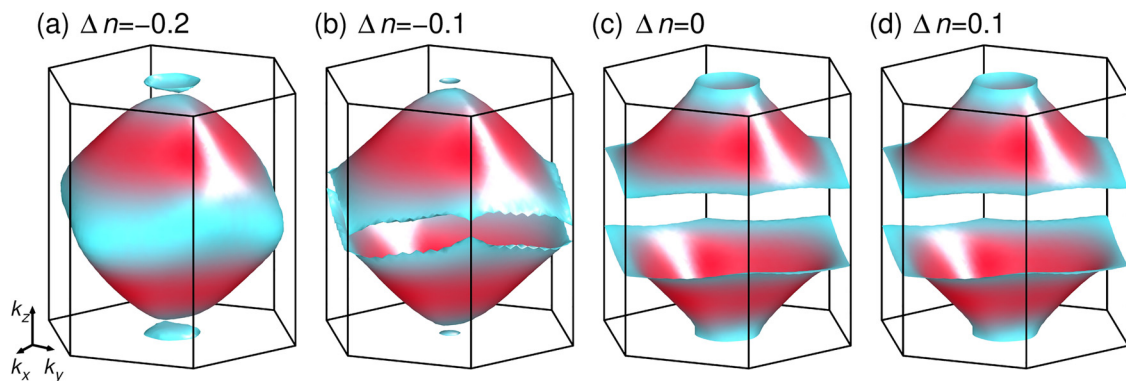


FIG. 2. Generalized gradient approximation (GGA) Fermi surfaces of $\text{Pb}_9\text{Cu}(\text{PO}_4)_6\text{O}$ for several doping levels $\Delta n = n - 7$. (c) is the Fermi surface of the stoichiometric compound, (a) and (b) correspond to hole doping of 0.2 and 0.1 electrons/f.u., and (d) shows electron doping of 0.1 electrons. Red (blue) indicates high (low) Fermi velocity as determined by full potential local orbital (FPLO).

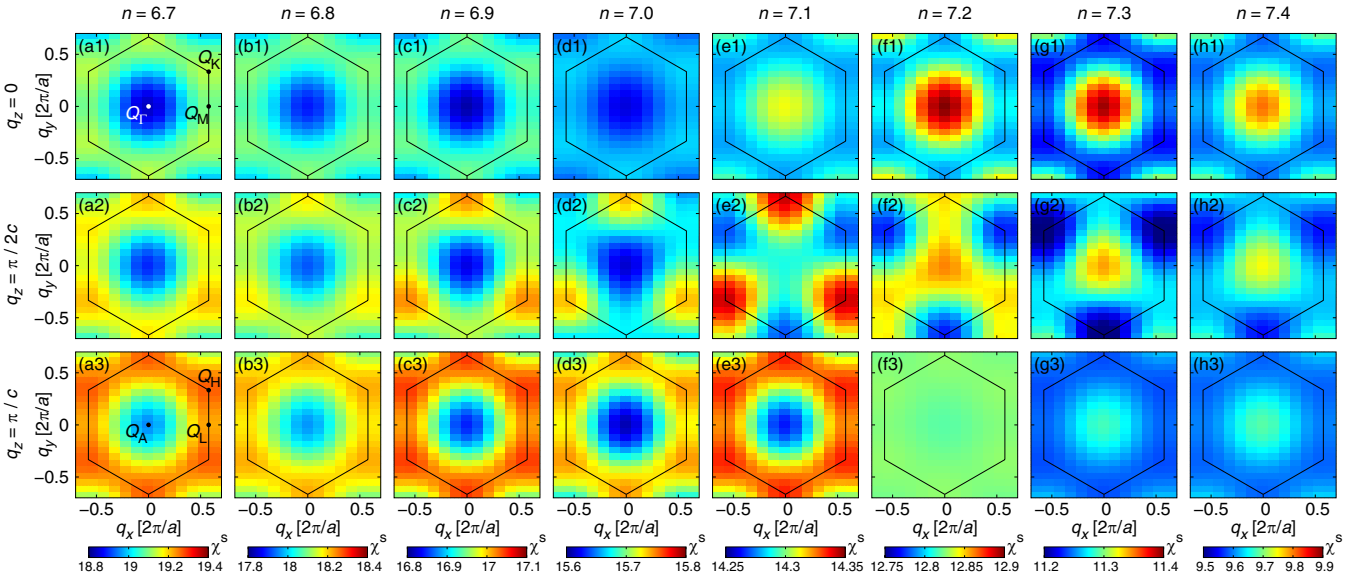


FIG. 3. Cuts through the static spin susceptibility $\chi^s(\mathbf{q})$ for (a) $q_z = 0$, (b) $q_z = \pi/2c$, and (c) $q_z = \pi/c$ at $T = 290$ K calculated within fluctuation exchange (FLEX). Interaction parameters are $U = 200$ meV, $V = U/2$, and $J = J' = U/4$. High-symmetry points are $\mathbf{Q}_\Gamma \equiv (0, 0, 0)$, $\mathbf{Q}_K \equiv (1/\sqrt{3}, \frac{1}{3}, 0)$, $\mathbf{Q}_M \equiv (1/\sqrt{3}, 0, 0)$, $\mathbf{Q}_A \equiv (0, 0, \frac{1}{2})$, $\mathbf{Q}_H \equiv (1/\sqrt{3}, \frac{1}{3}, \frac{1}{2})$, $\mathbf{Q}_L \equiv (1/\sqrt{3}, 0, \frac{1}{2})$, in units of $2\pi/a$ for the x and y components and of $2\pi/c$ for the z component. The high-symmetry points are shown in (a1) and (a3).

local interactions, which are represented by the Hamiltonian:

$$\mathcal{H}_{\text{int}} = \sum_i \left[\frac{U}{2} \sum_{\sigma} n_{i\sigma} n_{i\bar{\sigma}} + \frac{V}{2} \sum_{l \neq m} n_{il} n_{im} - \frac{J}{2} \sum_{l \neq m} \mathbf{S}_{il} \cdot \mathbf{S}_{im} + \frac{J'}{2} \sum_{l \neq m} \sum_{\sigma} c_{il\sigma}^\dagger c_{i\bar{l}\sigma}^\dagger c_{im\bar{\sigma}} c_{i\bar{m}\bar{\sigma}} \right], \quad (2)$$

where the orbital indices l and m run over two orbitals ($3d_{xz}$ and $3d_{yz}$) out of four. Here, U , V , J , and J' are intra-orbital Coulomb interaction, interorbital Coulomb interaction, Hund's coupling, and pair hopping, respectively.

We apply the FLEX approximation to the four-band Hubbard model. We change the electron number in the range of $6.5 \leq n \leq 7.5$. Note that, here, we are particularly interested in magnetic tendencies of doped materials as opposed to the stoichiometric compound that is insulating according to experiment [10] and theory [32–34]. We choose spin-rotation-invariant interaction parameters [35] $V = U/2$ and $J = J' = U/4$ for the Cu $3d$ orbitals, and we assume $U = 200$ meV. Using a much larger U value that might be expected for Cu $3d$ electrons would make calculations more difficult because of divergent spin susceptibilities but would not lead to different peak positions; therefore, we investigate the magnetic tendencies using a small U value. We use a $16 \times 16 \times 4$ \mathbf{k} mesh.

We discuss the momentum-dependent static spin susceptibility $\chi^s(\mathbf{q}) = \sum_{lm} \chi_{lm}^s(\mathbf{q})$, in which contributions from $3d_{xz}$ and $3d_{yz}$ orbitals are summed up. Figure 3 shows cuts of $\chi^s(\mathbf{q})$ at $q_z = 0, \pi/2c$, and π/c (zone boundary) for $6.7 \leq n \leq 7.4$. At the formal electron filling of $\text{Pb}_9\text{Cu}(\text{PO}_4)_6\text{O}$ ($n = 7.0$), $\chi^s(\mathbf{q})$ exhibits peaks at $\mathbf{q} = \mathbf{Q}_H$. This fluctuation corresponds to an antiferromagnetic (AFM) stacking of the 120° state on

the triangular lattice. The AFM fluctuation persists for hole doping. On the electron doping side, on the other hand, the magnetic properties change drastically. At $n = 7.1$, a peak is present at $\mathbf{q} = \mathbf{Q}_\Gamma$, which corresponds to the ferromagnetic (FM) fluctuation. The FM fluctuation becomes dominant for $n \gtrsim 7.2$.

Let us consider the origin of the AFM and FM fluctuations in $\text{Pb}_9\text{Cu}(\text{PO}_4)_6\text{O}$ in terms of a single-band Hubbard model on a triangular lattice. This model approximately describes the energy dispersion of the top band through Γ - M - K - Γ in Fig. 1. Figure 4 shows the spin susceptibility $\chi^s(\mathbf{q})$ for several values of the occupation number n . Here, n in this model corresponds to $n - 6$ in the four-band model of $\text{Pb}_9\text{Cu}(\text{PO}_4)_6\text{O}$. Also, $\chi^s(\mathbf{q})$ exhibits peaks at \mathbf{Q}_K around half-filling ($0.6 \leq n \leq 1.0$), while it has a peak at \mathbf{Q}_Γ near $\frac{3}{4}$ filling ($1.4 \leq n \leq 1.6$). These magnetic fluctuations can be understood well with the electronic structure. Around half-filling, the Fermi surface in the corresponding noninteracting system is a circle around the Γ point, as shown in Fig. 5(a). The nesting vector agrees with \mathbf{Q}_K , as indicated by the arrow in Fig. 5(a). On the other hand, the Fermi surface around $\frac{3}{4}$ filling is a hexagon inscribed in the first Brillouin zone, as shown in Fig. 5(b). The density of states is large at the M point because of the Van Hove singularity. Therefore, dominant particle-hole excitations occur in the \mathbf{q} vector that connects two M points, that is, $(2\pi/a, 0, 0)$, which corresponds to \mathbf{Q}_Γ . The Fermi surface thus explains AFM fluctuations corresponding to the 120° state for $n \lesssim 1$ and the strong FM fluctuations for $n \simeq 1.5$.

The variations of the magnetic properties between AFM and FM can be understood with the triangular lattice. However, $\text{Pb}_9\text{Cu}(\text{PO}_4)_6\text{O}$ shows two unique properties that the triangular lattice does not. First, the change from AFM to FM is very sensitive to electron doping. It is AFM at $n = 7.0$, and even with very small electron doping, it starts to be FM at

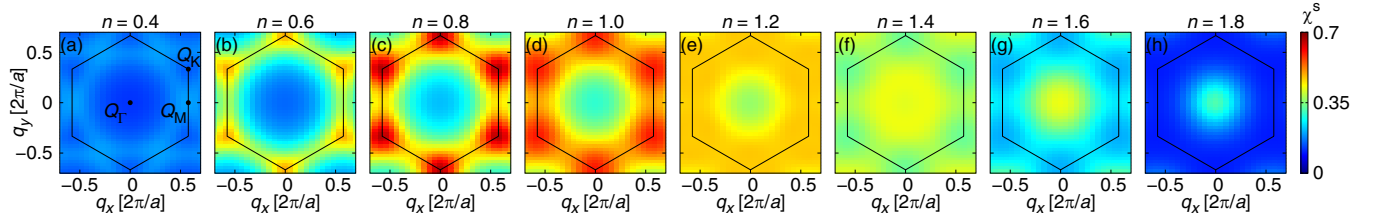


FIG. 4. The static spin susceptibility $\chi^s(\mathbf{q})$ of the triangular lattice at $T = |t|/4$ calculated within fluctuation exchange (FLEX). The interaction is $U = 9|t| = W$, where t is the nearest-neighbor hopping parameter, and W is the bandwidth. We use a 32×32 \mathbf{k} -mesh.

$n = 7.1$. Here, 0.1 electrons are needed to cause FM fluctuations when we start from stoichiometric integer filling. In the triangular lattice, on the other hand, 0.5 electrons are needed. Doping 0.5 electrons into a material is usually very difficult in reality. The second unique property of $\text{Pb}_9\text{Cu}(\text{PO}_4)_6\text{O}$ is the fact that ferromagnetism persists in the whole region of electron doping, while it disappears in the triangular lattice.

These two properties of $\text{Pb}_9\text{Cu}(\text{PO}_4)_6\text{O}$ result from the 3D Fermi surface. Even though the highest energy band is almost half-filled in total, various situations of filling are realized if we look into the 2D k path for different k_z : almost empty at $k_z = \pi/c$ and almost fully filled at $k_z = 0$, as shown in Fig. 6. Therefore, the Van Hove singularity at $(1/\sqrt{3}, 0, k_z)$ appears on the Fermi level even at the stoichiometric filling, and the FM fluctuation is enhanced by the mechanism discussed in Fig. 5(b). Moreover, when electrons are doped, the Fermi level passes the singularity point at a different k_z . This explains the result that the FM fluctuation is dominant in a wide range of electron doping levels in $\text{Pb}_9\text{Cu}(\text{PO}_4)_6\text{O}$.

Conclusions. We have studied the consequences of the electronic structure of $\text{Pb}_9\text{Cu}(\text{PO}_4)_6\text{O}$ for magnetic fluctuations. We find that, electronically, $\text{Pb}_9\text{Cu}(\text{PO}_4)_6\text{O}$ provides an interesting $\frac{3}{4}$ -filled, two-orbital triangular lattice Hamiltonian. As such, it can be partly understood from the one-band triangular lattice Hamiltonian that has previously been studied in the context of organic charge transfer salts and of sodium cobaltate. However, we have worked out two important differences that arise from the three-dimensionality of $\text{Pb}_9\text{Cu}(\text{PO}_4)_6\text{O}$, i.e., from the k_z dispersion of the electronic structure. One consequence is that the change of doping that triggers the transition between AFM and FM spin fluctuations is much smaller in $\text{Pb}_9\text{Cu}(\text{PO}_4)_6\text{O}$ than in the simple triangu-

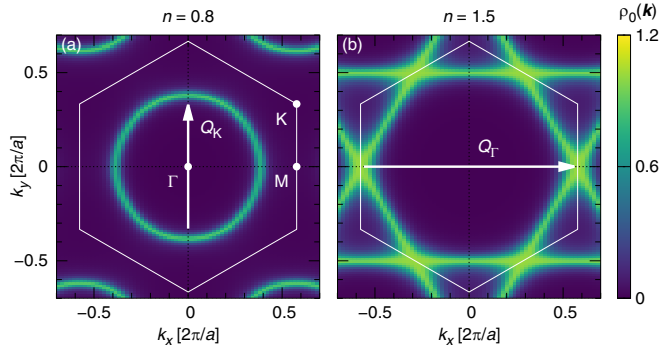


FIG. 5. Momentum-resolved density of states $\rho_0(\mathbf{k})$ at the Fermi level in a noninteracting triangular lattice model at $n = 0.8$ and 1.5. An artificial broadening of width $0.1t$ was applied.

lar lattice. The other consequence is that the FM fluctuations in the electron-doped region are significantly stabilized in the 3D two-orbital model.

While our FLEX result for the undoped material indicates AFM fluctuations, we also find that FM fluctuations are reached by very little electron doping. Thus, slightly inhomogeneous samples $\text{Pb}_{10-x}\text{Cu}_x(\text{PO}_4)_6\text{O}$ with $x \approx 1$ would have FM as well as AFM regions, and this could explain the levitation observed in some of the samples [2,5,9] of $\text{Pb}_9\text{Cu}(\text{PO}_4)_6\text{O}$.

By focusing on a single site for the position of the doped Cu^{2+} ion, we have introduced a significant simplification, just like in many other studies [20,21,23]. It is possible that disorder effects will play an important role in $\text{Pb}_9\text{Cu}(\text{PO}_4)_6\text{O}$ [24]. Nevertheless, in this paper, we show that the electronic structure that is present in slightly simplified $\text{Pb}_9\text{Cu}(\text{PO}_4)_6\text{O}$ has very interesting properties. It is characterized by two degenerate orbitals on a triangular lattice, $\frac{3}{4}$ filling, and a finite k_z dispersion. As this is a rather generic situation, it could already be realized in other existing materials, or it would not be too hard to design materials with this property. As the hope for superconductivity in $\text{Pb}_9\text{Cu}(\text{PO}_4)_6\text{O}$ is probably in vain, it makes sense to understand why and possibly find or design a similar material that supports a superconducting ground state. A likely disadvantage of $\text{Pb}_9\text{Cu}(\text{PO}_4)_6\text{O}$ is the large ratio between interaction strength on the d orbitals and the bandwidth [23]; in the search for a better $\text{Pb}_9\text{Cu}(\text{PO}_4)_6\text{O}$, wider bands or weaker local interactions would be desirable. If superconductivity could be realized in a dopable material

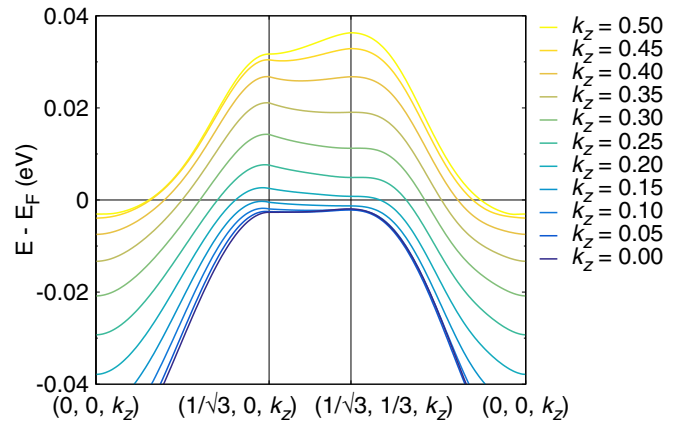


FIG. 6. Band structure of $\text{Pb}_9\text{Cu}(\text{PO}_4)_6\text{O}$ along a triangular k path for different values of k_z . The x and y components are in units of $2\pi/a$, and the z component is in units of $2\pi/c$. The path at $k_z = 0$ is equivalent to Γ - M - K - Γ .

with the electronic structure of $\text{Pb}_9\text{Cu}(\text{PO}_4)_6\text{O}$, then we would expect that the order parameter could be tuned between singlet and triplet.

Acknowledgments. We acknowledge useful discussions with S. Kasahara and K. Kobayashi. The computation in this paper was done using the facilities of the Supercomputer

Center, the Institute for Solid State Physics, the University of Tokyo. M.S. was supported by JSPS KAKENHI Grant No. 22H01181 and by Graduate School of Science, Kyoto University, under the Ginpu Fund. J.O. was supported by JSPS KAKENHI Grants No. 21H01041, No. 21H01003, and No. 23H04869.

- [1] S. Lee, J.-H. Kim, and Y.-W. Kwon, The first room-temperature ambient-pressure superconductor, [arXiv:2307.12008](#).
- [2] S. Lee, J. Kim, H.-T. Kim, S. Im, S. An, and K. H. Auh, Superconductor $\text{Pb}_{10-x}\text{Cu}_x(\text{PO}_4)_6\text{O}$ showing levitation at room temperature and atmospheric pressure and mechanism, [arXiv:2307.12037](#).
- [3] K. Kumar, N. K. Karn, and V. P. S. Awana, Synthesis of possible room temperature superconductor LK-99: $\text{Pb}_9\text{Cu}(\text{PO}_4)_6\text{O}$, *Supercond. Sci. Technol.* **36**, 10LT02 (2023).
- [4] Q. Hou, W. Wei, X. Zhou, Y. Sun, and Z. Shi, Observation of zero resistance above 100°K in $\text{Pb}_{10-x}\text{Cu}_x(\text{PO}_4)_6\text{O}$, [arXiv:2308.01192](#).
- [5] K. Guo, Y. Li, and S. Jia, Ferromagnetic half levitation of LK-99-like synthetic samples, *Sci. China Phys. Mech. Astron.* **66**, 107411 (2023).
- [6] K. Kumar, N. K. Karn, Y. Kumar, and V. P. S. Awana, Absence of superconductivity in LK-99 at ambient conditions, *ACS Omega* (2023), doi:[10.1021/acsomega.3c06096](#).
- [7] P. K. Jain, Superionic phase transition of copper(I) sulfide and its implication for purported superconductivity of LK-99, *J. Phys. Chem. C* **127**, 18253 (2023).
- [8] S. Zhu, W. Wu, Z. Li, and J. Luo, First order transition in $\text{Pb}_{10-x}\text{Cu}_x(\text{PO}_4)_6\text{O}$ ($0.9 < x < 1.1$) containing Cu_2S , [arXiv:2308.04353](#).
- [9] H. Wu, L. Yang, B. Xiao, and H. Chang, Successful growth and room temperature ambient-pressure magnetic levitation of LK-99, [arXiv:2308.01516](#).
- [10] P. Puphal, M. Y. P. Akbar, M. Hepting, E. Goering, M. Isobe, A. A. Nugroho, and B. Keimer, Single crystal synthesis, structure, and magnetism of $\text{Pb}_{10-x}\text{Cu}_x(\text{PO}_4)_6\text{O}$, *APL Mater.* **11**, 101128 (2023).
- [11] J. Lai, J. Li, P. Liu, Y. Sun, and X.-Q. Chen, First-principles study on the electronic structure of $\text{Pb}_{10-x}\text{Cu}_x(\text{PO}_4)_6\text{O}$ ($x = 0, 1$), *J. Mater. Sci. Technol.* **171**, 66 (2024).
- [12] S. M. Griffin, Origin of correlated isolated flat bands in copper-substituted lead phosphate apatite, [arXiv:2307.16892](#).
- [13] L. Si and K. Held, Electronic structure of the putative room-temperature superconductor $\text{Pb}_9\text{Cu}(\text{PO}_4)_6\text{O}$, *Phys. Rev. B* **108**, L121110 (2023).
- [14] R. Kurlito, S. Lany, D. Pashov, S. Acharya, M. van Schilfhaarde, and D. S. Dessau, Pb-apatite framework as a generator of novel flat-band CuO based physics, including possible room temperature superconductivity, [arXiv:2308.00698](#).
- [15] J. Cabezas-Escases, N. F. Barrera, C. Cardenas, and F. Munoz, Theoretical insight on the LK-99 material, [arXiv:2308.01135](#).
- [16] O. Tavakol and T. Scaffidi, Minimal model for the flat bands in copper-substituted lead phosphate apatite, [arXiv:2308.01315](#).
- [17] P. A. Lee and Z. Dai, Effective model for $\text{Pb}_9\text{Cu}(\text{PO}_4)_6\text{O}$, [arXiv:2308.04480](#).
- [18] M. M. Hirschmann and J. Mitscherling, Minimal model for double Weyl points, multiband quantum geometry, and singular flat band inspired by LK-99, [arXiv:2308.03751](#).
- [19] D. M. Korotin, D. Y. Novoselov, A. O. Shorikov, V. I. Anisimov, and A. R. Oganov, Electronic correlations in promising room-temperature superconductor $\text{Pb}_9\text{Cu}(\text{PO}_4)_6\text{O}$: A DFT+DMFT study, [arXiv:2308.04301](#).
- [20] L. Si, M. Wallerberger, A. Smolyanyuk, S. di Cataldo, J. M. Tomczak, and K. Held, $\text{Pb}_{10-x}\text{Cu}_x(\text{PO}_4)_6\text{O}$: A Mott or charge transfer insulator in need of further doping for (super)conductivity, *J. Phys. Condens. Matter* (2023), doi:[10.1088/1361-648X/ad0673](#).
- [21] C. Yue, V. Christiansson, and P. Werner, Correlated electronic structure of $\text{Pb}_{10-x}\text{Cu}_x(\text{PO}_4)_6\text{O}$, [arXiv:2308.04976](#).
- [22] H. Oh and Y.-H. Zhang, S-wave pairing in a two-orbital t - J model on triangular lattice: Possible application to $\text{Pb}_{10-x}\text{Cu}_x(\text{PO}_4)_6\text{O}$, [arXiv:2308.02469](#).
- [23] N. Witt, L. Si, J. M. Tomczak, K. Held, and T. Wehling, No superconductivity in $\text{Pb}_9\text{Cu}_1(\text{PO}_4)_6\text{O}$ found in orbital and spin fluctuation exchange calculations, [arXiv:2308.07261](#).
- [24] Y. Sun, K.-M. Ho, and V. Antropov, Metallization and spin fluctuations in Cu-doped lead apatite, [arXiv:2308.03454](#).
- [25] N. E. Bickers, D. J. Scalapino, and S. R. White, Conserving approximations for strongly correlated electron systems: Bethe-Salpeter equation and dynamics for the two-dimensional Hubbard model, *Phys. Rev. Lett.* **62**, 961 (1989).
- [26] H. Ikeda, R. Arita, and J. Kuneš, Phase diagram and gap anisotropy in iron-pnictide superconductors, *Phys. Rev. B* **81**, 054502 (2010).
- [27] K. Koepnick and H. Eschrig, Full-potential nonorthogonal local-orbital minimum-basis band-structure scheme, *Phys. Rev. B* **59**, 1743 (1999).
- [28] J. P. Perdew, K. Burke, and M. Ernzerhof, Generalized gradient approximation made simple, *Phys. Rev. Lett.* **77**, 3865 (1996).
- [29] K. Koepnick, O. Janson, Y. Sun, and J. van den Brink, Symmetry-conserving maximally projected Wannier functions, *Phys. Rev. B* **107**, 235135 (2023).
- [30] S. V. Krivovichev and P. C. Burns, Crystal chemistry of lead oxide phosphates: Crystal structures of $\text{Pb}_4\text{O}(\text{PO}_4)_2$, $\text{Pb}_8\text{O}_5(\text{PO}_4)_2$ and $\text{Pb}_{10}(\text{PO}_4)_6\text{O}$, *Z. Kristallogr.* **218**, 357 (2003).
- [31] Y. Jiang, S. B. Lee, J. Herzog-Arbeitman, J. Yu, X. Feng, H. Hu, D. Clugru, P. S. Brodale, E. L. Gormley, M. G. Vergniory *et al.*, $\text{Pb}_9\text{Cu}(\text{PO}_4)_6(\text{OH})_2$: Phonon bands, localized flat band magnetism, models, and chemical analysis, [arXiv:2308.05143](#).
- [32] D. Pashov, S. Acharya, S. Lany, D. S. Dessau, and M. van Schilfhaarde, Multiple Slater determinants and strong spin-fluctuations as key ingredients of the electronic

- structure of electron- and hole-doped $\text{Pb}_{10-x}\text{Cu}_x(\text{PO}_4)_6\text{O}$, [arXiv:2308.09900](#).
- [33] M. W. Swift and J. L. Lyons, Comment on “Origin of correlated isolated flat bands in copper-substituted lead phosphate apatite”, [arXiv:2308.08458](#).
- [34] J. Liu, T. Yu, J. Li, J. Wang, J. Lai, Y. Sun, X.-Q. Chen, and P. Liu, Symmetry breaking induced insulating electronic state in $\text{Pb}_9\text{Cu}(\text{PO}_4)_6\text{O}$, [Phys. Rev. B **108**, L161101 \(2023\)](#).
- [35] D. Guterding, H. O. Jeschke, P. J. Hirschfeld, and R. Valentí, Unified picture of the doping dependence of superconducting transition temperatures in alkali metal/ammonia intercalated FeSe, [Phys. Rev. B **91**, 041112\(R\) \(2015\)](#).